

A Novel Method for Uncertainty Inverse Problems and Application to Material Characterization of Composites

C. Jiang · G.R. Liu · X. Han

Received: 14 February 2007 / Accepted: 31 July 2007 / Published online: 22 August 2007
© Society for Experimental Mechanics 2007

Abstract A novel method is suggested to deal with so-called *uncertainty* inverse problems (UIPs) which are a class of inverse problems with uncertainty in the system parameters of the forward model. *Interval* which represents a closed bounded set of real numbers is used to model and characterize the uncertainty in our formulation, and hence only the bounds of the uncertainty of the system parameters are needed. For a specific input vector, the possible values of the outputs form an *interval vector* because of the uncertainty. An error function is defined using the measured interval vector of the outputs and those computed using a forward model. The UIP is then formulated as an optimization problem which minimizes the error function. To improve the optimization efficiency, an interval forward model is constructed based on the interval analysis method which can calculate very efficiently the bounds of the outputs caused by the uncertainty of the system parameters. The present method is applied to a complex inverse problem, namely material characterization of composite

laminates using elastic waves. Uncertainty of load is considered, and the hybrid numerical method (HNM) is used to compute the transient displacement responses. The engineering constants of two kinds of laminates are successfully identified using the simulated measurements of the outputs.

Keywords Uncertainty · Inverse problem · Interval · Optimization · Material characterization · Composite laminate

Introduction

Inverse problems can be defined as problems to estimate input through given output, in contrast with the forward problems concern the determination of output from input. Many problems in science and engineering should and can be formulated as inverse problems, such as identification of cracks and defects, estimation of boundary conditions on inaccessible boundary, and nondestructive evaluation of material property etc. Due to the advances of computer and computational technology, more and more complex design problems are needed to be solved through inverse analysis techniques. Therefore, inverse problems have been widely investigated and a great amount of literatures on this field have been published [e.g. 1–6]. However, most of the existing inverse analysis methods focus on deterministic problems in which all of the concerned parameters can be given in certain values. Thus for a specific input, a deterministic output can be obtained and hence the output can be in turn used to determine the input inversely. In practice, however, uncertainty exists in most of the practical engineering problems such as uncertainties of load, material property and geometrical dimension etc. In such *uncertain-*

C. Jiang · X. Han
State Key Laboratory of Advanced Design and Manufacturing for Vehicle Body, College of Mechanical and Automotive Engineering, Hunan University,
Changsha 410082, People's Republic of China

G.R. Liu
Centre for Advanced Computations in Engineering Science,
Department of Mechanical Engineering,
National University of Singapore,
10 Kent Ridge Crescent,
Singapore 119260, Singapore

G.R. Liu (✉)
Singapore–MIT Alliance (SMA),
E4-04-10, 4 Engineering Drive 3,
Singapore 117576, Singapore
e-mail: mpeliugr@nus.edu.sg

ty problems, the output is uncertain for a specific input, and hence it seems impossible to determine the input through only a “single” measurement of the output, as we usually do for deterministic inverse problems. This is because that a point-to-point “mapping” between the input and output is undermined by existence of the uncertainty. To obtain a reliable solution, issues concerning with the uncertainty must be investigated and a corresponding inverse analysis method should be developed.

Probability method [e.g. 7–11] is the most popular approach to model the uncertainty, and it has been widely studied and applied to practical engineering problems. This kind of method is based on precise probability distributions of the parameters with uncertainty. However, sufficient information on the uncertainty is not always available or sometimes expensive for many practical problems. Furthermore, there are researches indicating that even a small deviation of the probability distribution is likely to cause a large error of the reliability analysis [12].

In the recent two decades, the interval method in which *interval* is employed to model the uncertainty has been attracting more and more attentions [13–16]. Thus only the bounds of the uncertainty of a parameter are needed instead of a precise probability distribution, which can make the uncertainty analysis more convenient and economical. Interval method has been successfully applied to uncertainty optimization problems, and a kind of method called interval number programming has been developed. References [17–19] investigated the linear programming problems with interval coefficients in objective function. A programming method was proposed by Liu and Da [20] to solve the problems with interval coefficients in both of the objective function and constraints using the fuzzy constraint satisfactory degree. Based on a comparative study on ordering intervals, a linear interval number programming method was constructed [21]. A nonlinear interval number programming (NINP) problem was studied in which only the objective function with uncertainty was considered, and the problem was finally converted into a three-objective deterministic optimization problem [22]. A neural network was adopted to create an approximation between the design variables and the interval of the objective function, whereby an NINP method with high efficiency was suggested [23]. In NINP, generally, the nested optimization will be caused in which the outer optimization is used to optimize the design variables and the inner optimization is used to obtain the bounds of the objective function and constraints. To eliminate the nested optimization and improve the computation efficiency, a new NINP method was proposed by introducing the interval analysis method [24, 25]. The above works proved that interval method is effective for modeling the uncertainty and dealing with the uncertainty optimization problems. It is therefore natural to use

intervals to model the uncertainty in our formulation and formulate the UIPs as optimization problems.

In this paper, a new method is suggested to deal with *uncertainty* inverse problems (UIPs) in which the uncertainty of the system parameters is described by intervals. Thus for a specific combination of the inputs, the possible values of the outputs will form an interval vector. A measured interval vector of the outputs is then required, and the inverse analysis is performed to find an input vector which makes the uncertainty forward model produce exactly the measured interval vector. Thus the UIP is formulated as an optimization problem based on an error function. To avoid the *nested* optimization, an interval forward model is formulated based on the interval analysis method by which the bounds of the outputs caused by the uncertainty can be obtained very efficiently. Through interval forward model, the uncertainty of the system parameters is eliminated, and a deterministic “mapping” between the input vector and the interval vector of the outputs is created. In the application to material characterization of composite laminates using elastic waves, the hybrid numerical method (HNM) [26–30] is adopted to compute the transient displacement responses, and whereby an efficient interval forward model is constructed to compute the bounds of the transient displacement responses caused by the uncertainty in load. The intergeneration projection genetic algorithm (IPGA) [31] with a fine global convergence performance is employed as optimization solver. As an example, the determination of engineering constants of two kinds of composite laminates is carried out, and the numerical results demonstrate the effectiveness of the present method.

Uncertainty Inverse Problems

For a general deterministic engineering inverse problem, the forward model cannot be expressed explicitly and hence it can only be represented by a function as follows [5]:

$$Y = S(P_1, P_2, \dots, P_k, X) \quad (1)$$

where Y is a vector that collects all the outputs, S is the system matrix of functions of vectors parameters, P_1, P_2, \dots, P_k , and X is a vector that collects the inputs [5]. If the outputs of the system can be obtained by means of measurement, the inverse problem can be formulated as an optimization problem based on L_2 norm:

$$\min_{X \in \Omega} \sum_{i=1}^n (Y_i(X) - Y_i^m(X^t))^2 \quad (2)$$

which represents a least square sum of errors of the predicated outputs based on the forward model and an

assumed X with respect to the measured outputs Y^m . n Denotes the number of the measured sampling points. X^t is the inherent value of input vector X for the true system, and Ω is the inverse analysis space. Obviously, an ideal solution of X is X^t . From Fig. 1, it can be found that there exists a deterministic “mapping” between input vector X and output vector Y , thus we can inversely determine a unique X using a measurement of Y as long as the problem is “well-posed”.

For an *uncertainty* inverse problem (UIP), some system parameters are uncertain, and equation (1) can be changed to an *uncertainty* forward model:

$$Y = S_u(P_1, P_2, \dots, P_k, X, U) \tag{3}$$

where U is a q -dimensional uncertainty vector composed by the system parameters with uncertainty, and S_u is the system matrix of functions with uncertainty. Because of the uncertainty vector U , the output vector Y is also uncertain for a specific X . Thus the “mapping” relation between X and Y no longer exists, and a “single” measurement of Y is unable to contain the sufficient information to determine X precisely. The above UIP is more complex and difficult to solve than the deterministic inverse problems, and the traditional inverse analysis methods are incapable of dealing with this type of problems.

A Method for Uncertainty Inverse Problems Based on Intervals

First, an interval A^I is defined as follows [13]:

$$A^I = [A^L, A^R] = \{A | A^L \leq A \leq A^R\} \tag{4}$$

which represents a closed bounded set of real numbers. The superscript I denotes an interval, and L, R denote the lower and upper bounds of interval, respectively.

Here an interval vector U^I is used to model the uncertainty of U in equation (3):

$$U \in U^I = [U^L, U^R], U_i \in U_i^I = [U_i^L, U_i^R], i = 1, 2, \dots, q \tag{5}$$

which means that the possible values of each system parameter with uncertainty belong to an interval. Therefore for a specific X , the possible values of the output vector Y will form a following interval vector instead of a real

number vector as long as S_U is continuous with respect to the uncertainty vector U :

$$Y(X, U) \in Y^I(X) = [Y^L(X), Y^R(X)] \tag{6}$$

where $Y^I(X)$ is the interval vector of the outputs at X , and its bounds $Y^L(X)$ and $Y^R(X)$ can be rewritten as follows:

$$Y^L(X) = \min_{U \in \Gamma} Y(U, X), Y^R(X) = \max_{U \in \Gamma} Y(U, X) \tag{7}$$

$$\Gamma = \{U | U_i^L \leq U_i \leq U_i^R, i = 1, 2, \dots, q\}$$

Now in fact we have created a new deterministic relation between the input X and the interval vector $Y^I(X)$ through equations (6) and (7), namely a specific X corresponds to a deterministic interval vector $Y^I(X)$. In this relation, the information from the parameters with uncertainty is included. Thus the inverse analysis process for the considered UIP can be performed as follows:

1. Based on information of the uncertainty and engineering experience, specify the intervals of the system parameters with uncertainty;
2. Through enough times of experimental measurements or observations, an amount of diffused measurement data can be obtained for an output. Selecting the maximum and minimum values, the interval of this output can be also obtained. Thus for all of the outputs, we can achieve a measured interval vector $(Y^I)^m = [(Y^L)^m, (Y^R)^m]$.
3. Construct an uncertainty forward model using numerical methods such as the finite element method (FEM) to create the relation among X, U and Y .
4. Construct an optimization problem to inversely determine an X which makes the uncertainty forward model have an interval vector $(Y^I)^m$ of the outputs.

In this paper, the optimization problem is formulated based on the L_2 norm of the error function:

$$\min_{X \in \Omega} \sum_{i=1}^n [(Y_i^L(X) - (Y_i^L(X^t))^m)^2 + (Y_i^R(X) - (Y_i^R(X^t))^m)^2] \tag{8}$$

Equation (8) contains two parts of errors. One is the least square sum of errors of the computed lower bounds of the outputs with respect to the measured lower bounds, and the other is those of the upper bounds. Obviously, the ideal solution of X is also X^t for the above error function.

Figure 2 is a sketch of the inverse analysis of the UIPs based on intervals. The part enclosed by the rectangular framework can be regarded as a new kind of forward model (termed as “interval forward model”) which outputs an interval vector for an input vector X , instead of a real

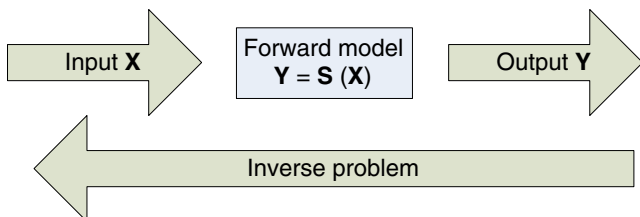


Fig. 1 Deterministic inverse problems [5]

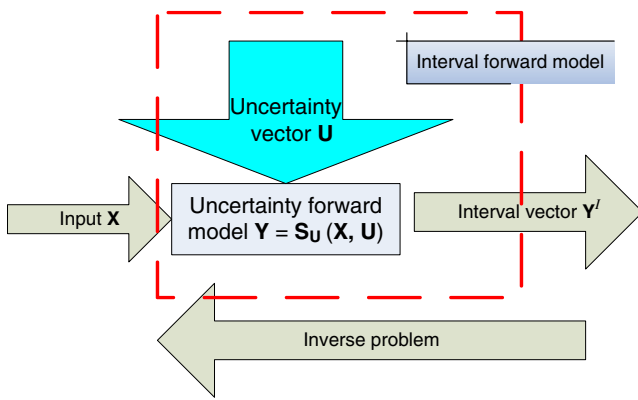


Fig. 2 Uncertainty inverse problems

number vector like the traditional deterministic inverse problems. If two optimization processes defined by equation (7) are employed as the interval forward model, a nested optimization will be inevitably caused when we optimize the error function equation (8), and the efficiency to solve such a nested problem will be unacceptable even for very simple UIPs. To avoid the nested optimization and improve the inverse analysis efficiency, an efficient interval forward model will be constructed based on the interval analysis method [32] in the following section.

An Interval Forward Model

Following the notation in interval mathematics [13], the interval vector U^I of the uncertainty vector can be rewritten in the following form:

$$\begin{aligned} U^I &= [U^L, U^R] = [U^c - U^w, U^c + U^w] \\ &= U^c + [-1, 1]U^w \end{aligned} \quad (9)$$

where U^c and U^w denote the midpoint vector and the radius vector of U^I , respectively:

$$U^c = \frac{U^L + U^R}{2}, \quad U_i^c = \frac{U_i^L + U_i^R}{2}, \quad i = 1, 2, \dots, q \quad (10)$$

$$U^w = \frac{U^R - U^L}{2}, \quad U_i^w = \frac{U_i^R - U_i^L}{2}, \quad i = 1, 2, \dots, q \quad (11)$$

Based on equation (9), the uncertainty vector U can be rewritten as:

$$U = U^c + \delta U \quad (12)$$

where

$$\delta U \in [-1, 1]U^w, \quad \delta U_i \in [-1, 1]U_i^w, \quad i = 1, 2, \dots, q \quad (13)$$

When the uncertainty levels, namely the intervals of the system parameters with uncertainty are relatively small (which is true for most of UIPs), the output vector $Y(X, U)$ in equation (3) can be approximated as a linear function with respect to δU based on the first-order Taylor expansion:

$$Y(X, U) = Y(X, U^c + \delta U) \approx Y(X, U^c) + \sum_{j=1}^q \frac{\partial Y(X, U^c)}{\partial U_j} \delta U_j \quad (14)$$

As δU belongs to an interval vector defined by equation (13), the interval vector of $Y(X, U)$ caused by the uncertainty can be obtained through a natural interval extension of equation (14) [13, 32]:

$$Y^I(X) = Y(X, U^c) + \sum_{j=1}^q \frac{\partial Y(X, U^c)}{\partial U_j} [-1, 1]U_j^w \quad (15)$$

Then the lower bound vector $Y^L(X)$ and the upper bound vector $Y^R(X)$ of the outputs at specific X can be obtained explicitly:

$$Y^L(X) = \min_{U \in \Gamma} Y(X, U) = Y(X, U^c) - \sum_{j=1}^q \left| \frac{\partial Y(X, U^c)}{\partial U_j} \right| U_j^w \quad (16)$$

$$Y^R(X) = \max_{U \in \Gamma} Y(X, U) = Y(X, U^c) + \sum_{j=1}^q \left| \frac{\partial Y(X, U^c)}{\partial U_j} \right| U_j^w \quad (17)$$

In equations (16) and (17), $Y(X, U^c)$ can be achieved directly through one evaluation of the uncertainty forward model at X and U^c . The derivatives of Y with respect to the system parameters with uncertainty can be calculated through different methods according to the practical problems. For problems with uncertainty forward model in explicit expressions, the derivatives can also be obtained explicitly; for problems with implicit expressions, the derivatives can be calculated analytically based on numerical algorithms such as FEM [e.g. 32], or numerical differentiation techniques such as central-difference approximation and forward-difference approximation [33]. Using the above interval forward model, the interval vector of the outputs can be obtained analytically or though only a very small number of evaluations of the uncertainty forward model, and hence the time-consuming nested optimization can be avoided for equation (8).

Optimization Process

Based on the interval forward model, the optimization problem defined by equation (8) for an uncertainty inverse problem can be written as follows:

$$\min_{\mathbf{X} \in \Omega} \sum_{i=1}^n \left[(Y_i^L(\mathbf{X}) - (Y_i^L(\mathbf{X}^t))^m)^2 + (Y_i^R(\mathbf{X}) - (Y_i^R(\mathbf{X}^t))^m)^2 \right] \tag{18}$$

where

$$Y_i^L(\mathbf{X}) = \min_{\mathbf{U} \in \Gamma} Y_i(\mathbf{X}, \mathbf{U}) = Y_i(\mathbf{X}, \mathbf{U}^c) - \sum_{j=1}^q \left| \frac{\partial Y_i(\mathbf{X}, \mathbf{U}^c)}{\partial U_j} \right| U_j^w, \quad i = 1, 2, \dots, q$$

$$Y_i^R(\mathbf{X}) = \max_{\mathbf{U} \in \Gamma} Y_i(\mathbf{X}, \mathbf{U}) = Y_i(\mathbf{X}, \mathbf{U}^c) + \sum_{j=1}^q \left| \frac{\partial Y_i(\mathbf{X}, \mathbf{U}^c)}{\partial U_j} \right| U_j^w, \quad i = 1, 2, \dots, q$$

Equation (18) is actually a deterministic optimization problem as the uncertainty has been eliminated by the interval forward model, and it can be solved by traditional nonlinear optimization techniques. The iterative process of the optimization is shown in Fig. 3. For an input vector of each iterative step, the interval vector of the outputs caused by the uncertainty can be calculated by interval forward model. Then integrated with the measured interval vector, the error function can be also calculated. The iterative process will be terminated until a stopping criterion is satisfied.

Application to Material Characterization of Composite Laminates

The present method is now used to identify the material property of a composite laminate composed of many layers with different fiber orientations, as shown in Fig. 4. This

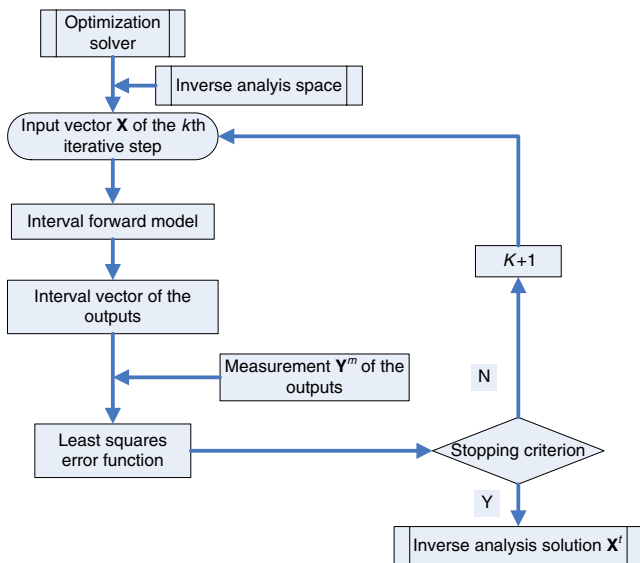


Fig. 3 Inverse analysis process for uncertainty inverse problems

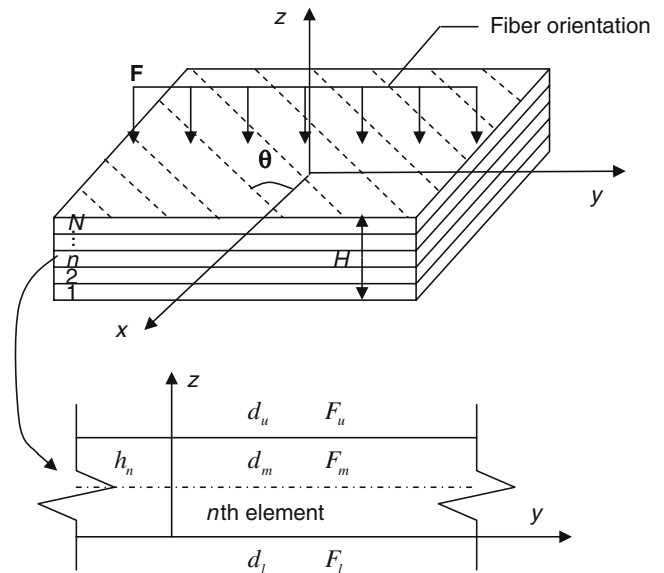


Fig. 4 An anisotropic composite laminate [5]

application is in part based on the previous works of Liu and Han [5], Liu et al. [34], and Han and Liu [35] on material determination of composites using elastic waves. In these works, the load applied to the plate is deterministic. However, in practical applications, it is commonly difficult to generate a deterministic load because of the instability of the exciter, especially for the high-frequency loads in wave propagation problems. Thus in our formulation, the load is treated as uncertain and the uncertainty inverse analysis process is performed as follows:

- Step 1 A dynamic load with a given time history is applied on the laminate;
- Step 2 Through enough times of experimental measurements, the bounds of the transient displacement responses at one receiving point can be obtained. Then an interval vector of the displacement responses corresponding to all of the sampling time points can be obtained as the measured interval vector of the outputs;
- Step 3 An error function is created based on the computed interval vector and the measured interval vector of the outputs, and an optimization solver is adopted to minimize the error function to determine the engineering constants of the laminate.

In this application, a vertical line sine load [5] is applied at $x=0$ on the upper surface of the plate as follows:

$$F = F_1(t)\delta(x)Q \tag{19}$$

where

$$F_1(t) = \begin{cases} \sin(2\pi t/t_d), & 0 \leq t \leq t_d \\ 0, & t < 0 \text{ and } t > t_d \end{cases} \tag{20}$$

where t_d is the time duration of the incident wave and equation (20) implies that the time history of the incident wave is only one cycle of sine function. Q is a constant amplitude. Here, the parameters t_d and Q are uncertain, and their uncertainty is modeled by intervals:

$$t_d \in t_d^I = [t_d^L, t_d^R], Q \in Q^I = [Q^L, Q^R] \tag{21}$$

The hybrid numerical method (HNM) [26–30] is employed to compute the transient displacement responses of the composite laminate, and it will be introduced firstly in the following section. Then based on HNM, an interval forward model will be constructed. Because the line load is used, the computation can be simplified as a two-dimensional problem and hence all of the quantities with respect to y are eliminated.

Hybrid Numerical Method

The HNM has been proved very effective for calculation of the transient responses of a laminated plate subjected to an incident wave. It was developed based on the early works on wave propagation problems [36–38]. As shown in Fig. 4, the plate is divided into N layer elements. H is the thickness of the plate and h_n is the thickness of the n th element. Each element is composed of three nodal planes and d_l, d_m, d_u denote the displacement vectors at the lower, middle and upper surfaces, respectively. θ is the ply orientation vector. Using the principle of virtual work, a set of approximate partial differential equations for an element are obtained. After assembling the matrixes of adjacent elements, the dynamic equilibrium equation of the whole plate is formulated as follows [26]:

$$F(x, t) = K_D d(x, t) + M \ddot{d}(x, t) \tag{22}$$

where

$$K_D = -A_1 \frac{\partial^2}{\partial^2 x} + A_4 \frac{\partial}{\partial x} + A_6 \tag{23}$$

where F is the load vector and M is the mass matrix. K_D is a differential operator matrix for the plate. The expressions of the matrixes A_1, A_4 and A_6 can refer to literature [26]. d is the transient displacement response vector on the nodal planes and “.” denotes the differentiation with respect to time t . The Fourier transformation is applied with respect to the horizontal coordinate x as follows:

$$\tilde{d}(k_x, t) = \int_{-\infty}^{+\infty} d(x, t) e^{ik_x x} dx \tag{24}$$

where the real transformation parameters k_x is wave number corresponding to the horizontal coordinate x . Applying equations (24) to (22) yields:

$$\tilde{F} = M \ddot{\tilde{d}} + K \tilde{d} \tag{25}$$

$$K = k_x^2 A_1 - i k_x A_4 + A_6 \tag{26}$$

where $\tilde{F}, \ddot{\tilde{d}}$ and \tilde{d} are Fourier transformations of F, \ddot{d} and d , respectively. Using the modal analysis method and Duhamel integration technique, the displacement response vector \tilde{d} in Fourier transformation domain can be obtained for different k_x . Finally the transient responses in space-time domain can be obtained using the following inverse Fourier transformation:

$$d(x, t) = \left(\frac{1}{2\pi}\right)^2 \int_{-\infty}^{+\infty} \tilde{d}(k_x, t) e^{-ik_x x} dk_x \tag{27}$$

Interval Forward Model Based on Hybrid Numerical Method

The bounds of the transient displacement responses d caused by the uncertainty in load can be obtained based on equations (16) and (17):

$$d^L(C, t) = \min_{(t_d, Q) \in \Gamma} d(C, t_d, Q, t) = d(C, t_d^c, Q^c, t) - \left| \frac{\partial d(C, t_d^c, Q^c, t)}{\partial t_d} \right| t_d^w - \left| \frac{\partial d(C, t_d^c, Q^c, t)}{\partial Q} \right| Q^w \tag{28}$$

$$d^R(C, t) = \max_{(t_d, Q) \in \Gamma} d(C, t_d, Q, t) = d(C, t_d^c, Q^c, t) + \left| \frac{\partial d(C, t_d^c, Q^c, t)}{\partial t_d} \right| t_d^w + \left| \frac{\partial d(C, t_d^c, Q^c, t)}{\partial Q} \right| Q^w \tag{29}$$

where C denotes the engineering constant vector of the laminate. In equations (28) and (29), $d(C, t_d^c, Q^c, t)$ can be

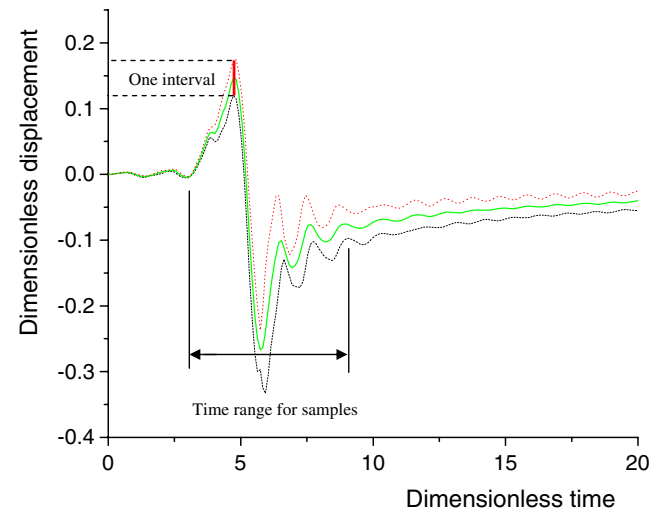


Fig. 5 Time history bounds of the transient responses caused by the uncertainty in load



Table 1 Search space of IP-GA for the engineering constants of glass/epoxy laminate

Parameter	True value	Search range	Possibility	Binary digit
E_1 (GPa)	38.48	[19.24, 57.72]	1,024	10
E_2 (GPa)	9.38	[4.89, 14.07]	1,024	10
G_{12} (GPa)	3.41	[1.71, 5.12]	1,024	10
ν_{12}	0.292	[0.15, 0.44]	1,024	10
ν_{23}	0.507	[0.25, 0.76]	1,024	10

calculated through one evaluation of HNM, and the first derivatives of the transient responses can be computed through differentiating both sides of equation (22) with respect to the parameters with uncertainty [39]:

$$\frac{\partial F(x, t_d^c, Q^c, t)}{\partial t_d} = K_D \frac{\partial d(x, C, t_d^c, Q^c, t)}{\partial t_d} + M \frac{\partial \ddot{d}(x, C, t_d^c, Q^c, t)}{\partial t_d} \quad (30)$$

$$\frac{\partial F(x, t_d^c, Q^c, t)}{\partial Q} = K_D \frac{\partial d(x, C, t_d^c, Q^c, t)}{\partial Q} + M \frac{\partial \ddot{d}(x, C, t_d^c, Q^c, t)}{\partial Q} \quad (31)$$

where $\frac{\partial F(x, t_d^c, Q^c, t)}{\partial t_d}$ can be obtained explicitly based on equations (19) and (20). Referring to $\frac{\partial F(x, t_d^c, Q^c, t)}{\partial t_d}$ and $\frac{\partial F(x, t_d^c, Q^c, t)}{\partial Q}$ as new load vectors, $\frac{\partial d(x, t_d^c, Q^c, t)}{\partial t_d}$ and $\frac{\partial d(x, C, t_d^c, Q^c, t)}{\partial Q}$ can be calculated through two evaluations of HNM. As a result, the interval forward model needs only three evaluations of HNM to compute the bounds of the transient displacement responses.

Optimization Solver

The intergeneration projection genetic algorithm (IP-GA) [31] is adopted as optimization solver. IP-GA combines micro GA (μ GA) with the intergeneration projection (IP) operator, and has a fine global convergence performance. The main difference between μ GA and traditional GAs is the size of

population and the mechanism that maintains the genetic diversity. In general, the population size of μ GA is very small (5~8). The IP operator aims to find a better individual by jumping along the move direction of the best individuals at two consecutive generations so as to improve the convergence rate. Generally, the generations of IP-GA that reach a global optimum are only 6.4~74.4% of μ GA [31].

Numerical Results and Discussion

A laminate $[-45/0/45/90^\circ]_s$, consisting of eight glass/epoxy layers symmetrically stacked is firstly investigated. The receiving point of transient responses is located at $x=2.0H$ on the upper surface of the laminate. The midpoints of the parameters t_d and Q are 2.0 and 1.0, respectively. The uncertainty levels of these two parameters are both $\pm 10\%$ off from the midpoints, namely:

$$t_d \in t_d^I = [1.8, 2.2], Q \in Q^I = [0.9, 1.1] \quad (32)$$

In the analysis, the dimensionless parameters defined by Liu et al. [26] are used. In this application, the simulated measurement of the outputs are used to determine the engineering constants of the composite plate, instead of the actual experimental measurement. Inputting the actual engineering constants into the interval forward model, we can obtain the bounds of the transient responses at the receiving point, as shown in Fig. 5. The dash line, solid line and dot line are lower bound, midpoint, and upper bound of the transient displacement responses, respectively. A time range is designated for samples. In this range, 15 time points are selected evenly, and for each time point we have an interval of the displacement responses. Thus a 15-dimensional interval vector of the transient responses can be obtained, and this computer-generated interval vector is used as a noise-free measurement of the outputs to determine the engineering constants of the laminate. Furthermore, a Gauss noise is directly added to the computer-generated interval vector to simulate the noise-contaminated measurement. A vector of pseudorandom number is generated from a Gauss distribution with mean a and standard deviation b using the Box–Muller method

Table 2 Inverse analysis results of glass/epoxy laminate

Engineering constant	True value	Noise free		1% Noise		3% Noise		5% Noise	
		Result	Error (%)	Result	Error (%)	Result	Error (%)	Result	Error (%)
E_1 (GPa)	38.48	38.72	0.75	39.85	3.56	40.91	6.31	40.94	6.39
E_2 (GPa)	9.38	9.29	0.96	9.20	1.92	9.33	0.53	9.52	1.49
G_{12} (GPa)	3.41	3.48	2.05	3.58	4.99	3.55	4.11	3.42	0.29
ν_{12}	0.292	0.287	1.71	0.298	2.05	0.314	7.53	0.355	21.6
ν_{23}	0.507	0.513	1.18	0.536	5.72	0.542	6.90	0.573	13.0



Table 3 Search space of IP-GA for the engineering constants of carbon/epoxy laminate

Parameter	True value	Search range	Possibility	Binary digit
E_1 (GPa)	142.17	[71.1, 213.3]	1,024	10
E_2 (GPa)	9.255	[4.6, 13.9]	1,024	10
G_{12} (GPa)	4.795	[2.4, 7.2]	1,024	10
ν_{12}	0.334	[0.167, 0.501]	1,024	10
ν_{23}	0.4562	[0.228, 0.684]	1,024	10

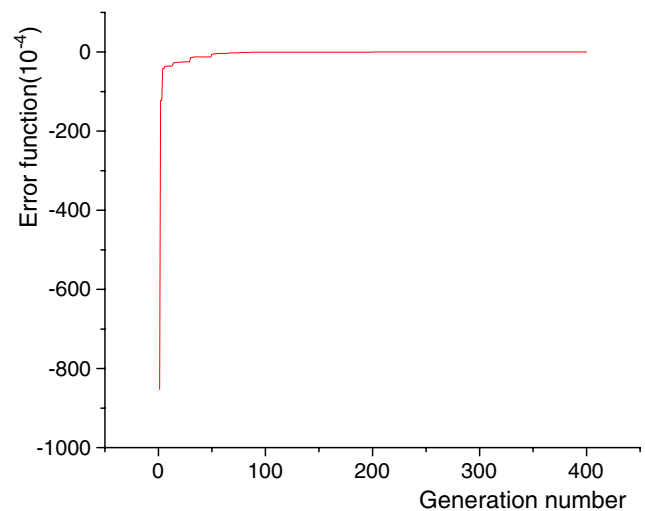
[40]. Here, the mean a is set to zero, and the standard deviation b is defined as follow [41]:

$$b = p_e \times \sqrt{\frac{\sum_{i=1}^{15} (u_i^m)^2}{15}} \quad (33)$$

where u_i^m is the computer-generated displacement lower bounds or upper bounds of the 15 sampling time points. Thus two vectors of pseudorandom number from two Gauss distributions with different standard deviations should be generated for the lower bound vector and upper bound vector of the outputs, respectively. p_e is a parameter to control the level of the noise contamination, for example, $p_e=0.01$ means 1% noise.

As shown in Table 1, the search space of the five engineering constants are set to $\pm 50\%$ off from the true values in the optimization process, and in IP-GA they are discretized and translated into a chromosome of 50 bits length according to the binary coding procedure. Thus there are a total of 2^{50} possible combinations of individuals. The population size and the probability of crossover for IP-GA are set to 5 and 0.5, respectively. A generation number 400 is used as the stopping criterion.

The inverse analysis results under the noise-free and different levels' noise-contaminated measurements of the outputs are listed in Table 2. It can be found that a very fine identification result can be obtained for the noise-free measurement, and the largest error with respect to the true value is only 2.05% which occurs in the engineering constant G_{12} . For the noisy measurements with noise levels

**Fig. 6** Convergence performance of IP-GA for the noise-free measurement

1 and 3%, the identification precision declines, and the largest errors of the engineering constants reach 5.72 and 7.53%, respectively. However, these results are still acceptable for an engineering problem. For the 5% noise-contaminated measurement, the identification result becomes unacceptable as the error of ν_{12} increases to a large value 21.6%. From Table 2, it can be also found that the engineering constants ν_{12} and ν_{23} are more sensitive to the noises of the measurements than E_1 , E_2 and G_{12} .

A laminate consisting of eight carbon/epoxy layers with a symmetrical stacking sequence $[-45/0/45/90]_s$ is also investigated, and it has a much stronger anisotropy than glass/epoxy layers. The search space of the five engineering constants are also set to $\pm 50\%$ off from the true values in the optimization process, as shown in Table 3. The chromosome length, generation number, population size and probability of crossover for IP-GA are set as same as the preceding case.

The inverse analysis results under the noise-free and different levels' noise-contaminated measurements are listed in Table 4. It is found that the identification results have a relatively fine precision for the noise-free and 1% noise-contaminated measurements. However, the unaccept-

Table 4 Inverse analysis results of carbon/epoxy laminate

Engineering constant	True value	Noise free		1% Noise		3% Noise		5% Noise	
		Result	Error (%)	Result	Error (%)	Result	Error (%)	Result	Error (%)
E_1 (GPa)	142.17	142.13	0.03	145.47	2.32	151.86	6.82	160.90	13.2
E_2 (GPa)	9.255	9.255	0.00	9.227	0.30	9.182	0.80	8.982	2.95
G_{12} (GPa)	4.795	4.793	0.04	4.751	0.92	4.666	2.69	4.751	0.92
ν_{12}	0.334	0.329	1.50	0.356	6.50	0.500	49.7	0.501	50.0
ν_{23}	0.4562	0.4564	0.04	0.452	0.92	0.443	2.89	0.435	4.21

able results are obtained for the 3 and 5% noise-contaminated measurements, as the largest errors of the engineering constants reach 49.7 and 50.0%, respectively. The results also show that v_{12} is much more sensitive to noises of the measurements than the other engineering constants. The convergence curve of IP-GA for the noise-free measurement is shown in Fig. 6 which shows that IP-GA has a fine convergence performance.

In practical applications of material determination of composite laminates, some points should be noticed. Firstly, in theory the receiving point can be arbitrarily located on the laminate surface and different receiving points should not result in much different results. However, there exists attenuation of signals in real structures, and an accurate numerical algorithm should be developed which takes into account the attenuation if the receiving point is far away from the excitation point. Secondly, to avoid the boundary effects, the receiving point should be far enough away from the boundary to enable the complete record of the full range of the transient displacement responses, before the arrival of the waves reflected by the boundary. Thirdly, the noises of the measurements should be ensured to be of small levels, as some of the material properties may be sensitive to the noises.

Conclusion

In this paper, a novel method is proposed to solve the *uncertainty* inverse problems (UIPs). The uncertainty is modeled using intervals, and it enables the uncertainty analysis very convenient and economical. The inverse analysis process is formulated as an optimization problem based on an error function. An interval forward model is constructed based on the interval analysis method, and hence the nested optimization is avoided. The present method is applied to the material characterization of the composite laminates subjected to a load with uncertainty which is a very complex UIP. An interval forward model is formulated using the hybrid numerical method (HNM), and it can compute the bounds of the transient responses only through a very small number of evaluations of HNM. Two kinds of composite laminates are investigated based on the simulated measurements of the outputs, and the results indicate that: fine identification results of the engineering constants can be obtained for the noise-free and small levels' noise-contaminated measurements of the outputs; some of the engineering constants are more sensitive to measurement noises than the others. Thus in practical applications of the present method to such problems that some inputs are sensitive to noises of the outputs, the noise level of the measurement should be ensured to be small through precise experiment and enough times of observations.

Acknowledgements This work is supported by the national 973 program under the Grant No. 2004CB719402, the program for Century Excellent Talents in University (NCET-04-0766), the National Natural Science Foundation of China (10572048) and the National Science Fund for Distinguished Young Scholars (50625519).

References

1. Tarantola A (1987) Inverse problem theory. Elsevier Science, The Netherlands.
2. Kubo S (ed) (1992) Inverse problems. Atlanta Technology Publications, Atlanta.
3. Santamarina JC, Fratta D (1998) Introduction to discrete signals and inverse problems in civil engineering. ACES, Reston.
4. Engl HW, Hanke M, Neubauer A (2000) Regularization of inverse problems. Kluwer, The Netherlands.
5. Liu GR, Han X (2003) Computational inverse techniques in nondestructive evaluation. CRC, Florida.
6. Liu GR, Han X, Xu YG, Lam KY (2001) Material characterization of functionally graded material by means of elastic waves and a progressive-learning neural network. Compos Sci Technol 61:1401–1411.
7. Charnes A, Cooper WW (1959) Chance-constrained programming. Manage Sci 6:73–79.
8. Kall P (1982) Stochastic programming. Eur J Oper Res 10:125–130.
9. Liu B, Iwamura K (1997) Modelling stochastic decision systems using dependent-chance programming. Eur J Oper Res 101(1):193–203.
10. Liu BD, Zhao RQ, Wang G (2003) Uncertain programming with applications. Tsinghua University Press, Beijing, China.
11. Abbas M, Bellahcene F (2006) Cutting plane method for multiple objective stochastic integer linear programming. Eur J Oper Res 168(3):967–984.
12. Ben-Haim Y, Elishakoff I (1990) Convex models of uncertainties in applied mechanics. Elsevier Science, Amsterdam.
13. Moore RE (1979) Methods and applications of interval analysis. Prentice-Hall, London.
14. Kreinovich V, Beck J, Ferregut C, Sanchez A, Keller GR, Averill M, Starks SA (2007) Monte-Carlo-type techniques for processing interval uncertainty, and their potential engineering applications. Reliab Comput 13(1):25–69.
15. Jerrell ME (1997) Interval arithmetic for input–output models with inexact data. Comput Econ 10(1):89–100.
16. Braems I, Ramdani N, Boudenne A, Kieffer M, Jaulin L, Ibos L, Walter E, Candau Y (2005) New set-membership techniques for parameter estimation in presence of model uncertainty. Proceedings of the 5th International Conference on Inverse Problems in Engineering: Theory and Practice, B09, Cambridge, UK.
17. Tanaka H, Ukuda T, Asal K (1984) On fuzzy mathematical programming. J Cybern 3:37–46.
18. Ishibuchi H, Tanaka H (1990) Multiobjective programming in optimization of the interval objective function. Eur J Oper Res 48:219–225.
19. Rommelfanger H (1989) Linear programming with fuzzy objective. Fuzzy Sets Syst 29:31–48.
20. Liu XW, Da QL (1999) A satisfactory solution for interval number linear programming. J Syst Eng 14:123–128 (China).
21. Sengupta A, Pal TK, Chakraborty D (2001) Interpretation of inequality constraints involving interval coefficients and a solution to interval linear programming. Fuzzy Sets Syst 119:129–138.
22. Ma LH (2002) Research on method and application of robust optimization for uncertain system. Ph.D. thesis, Zhejiang University, China.

23. Jiang C, Han X, Liu GR, Li GY (2007) The optimization of the variable binder force in U-shaped forming with uncertain friction coefficient. *J Mater Process Technol* 182:262–267.
24. Jiang C, Han X, Guan FJ (2006) A nonlinear structural optimization method based on interval description of uncertainty. *The Fourth China–Japan–Korea Joint Symposium on Optimization of Structural and Mechanical Systems*, Kunming, China, pp 347–352.
25. Jiang C, Han X, Guan FJ, Li YH (2007) An uncertain structural optimization method based on nonlinear interval number programming and interval analysis method. *Engineering Structures* DOI 10.1016/j.engstruct.2007.01.020.
26. Liu GR, Tani J, Ohyoshi T, Watanabe K (1991) Transient waves in anisotropic laminated plates, part1: theory. *J Vib Acoust* 113:230–234.
27. Liu GR, Tani J, Ohyoshi T, Watanabe K (1991) Transient waves in anisotropic laminated plates, part1: theory; part2: application. *J Vib Acoust* 113:235–239.
28. Liu GR, Lam KY, Tani J (1995) An exact method for analyzing elastodynamic responses of anisotropic laminates to line loads. *Mech Compos Mater Struct* 2:227–241.
29. Liu GR, Lam KY, Ohyoshi T (1997) A technique for analyzing elastodynamic responses of anisotropic laminated plates to line loads. *Compos B Eng* 28B:667–677.
30. Liu GR, Xi ZC (2002) *Elastic waves in anisotropic laminates*. CRC Press, Florida.
31. Xu YG, Liu GR, Wu ZP (2001) A novel hybrid genetic algorithm using local optimizer based on heuristic pattern move. *Appl Artif Intell* 15(7):601–631.
32. Qiu ZP, Wang XJ (2003) Comparison of dynamic response of structures with uncertain non-probabilistic interval analysis method and probabilistic approach. *Int J Solids Struct* 40:5423–5439.
33. Haftka RT, Gurdal Z (1992) *Elements of structural optimization*. Kluwer, The Netherlands.
34. Liu GR, Ma WB, Han X (2002) An inverse procedure for determination of material constants of composite laminates using elastic waves. *Comput Methods Appl Mech Eng* 191:3543–3554.
35. Han X, Liu GR (2003) Computational inverse technique for material characterization of functionally graded materials. *AIAA J* 41(2):288–295.
36. Waas G (1972) *Linear two-dimensional analysis of soil dynamics problems in semi-infinite layer media*. Ph.D. thesis, University of California, Berkeley, CA.
37. Nelson RB, Dong SB, Kalra RD (1971) Vibrations and waves in laminated orthotropic circular cylinders. *J Sound Vib* 18:429.
38. Kausel E (1986) Wave propagation in anisotropic layered media. *Int J Numer Methods Eng* 23:1567.
39. Han X, Jiang C, Huang YH (2006) Transient waves in composite laminated plates with uncertain load and material property. *Int J Numer Methods Eng* (in press).
40. Kendall MG, Stuart A (1969) *The advanced theory of statistics*. Griffin, London.
41. D’Cruz J, Crisp JDC, Ryall TG (1992) On the identification of a harmonic force on a viscoelastic plate from response data. *J Appl Mech–T ASME* 59:722–729.